PCCP

Accepted Manuscript

ROYAL SOCIETY OF CHEMISTRY

www.rsc.org/pccp

CREATED USING THE RSC LaTeX PCCP ARTICLE TEMPLATE – SEE www.rsc.org/electronicfiles FOR DETAILS

ARTICLE TYPE www. rsc.org/xxxxxx | XXXXXXXX

On the urea induced hydrophobic collapse of a water soluble polymer

Francisco Rodríguez-Ropero[a] and Nico F. A. van der Vegt[a]*

Received Xth XXXXXXXXXX 20XX, Accepted Xth XXXXXXXXX 20XX

First published on the web Xth XXXXXXXXXX 200X

DOI: 10.1039/b000000x

Stabilization of macromolecular folded states in solution by protective osmolytes has been traditionally explained on the basis of preferential osmolyte depletion from the macromolecule's first solvation shell. However recent theoretical and experimental studies suggest that protective osmolytes may directly interact with the macromolecule. An example is the stabilization of the collapsed globular state of Poly(N-isopropylacrylamide) (PNiPAM) by urea in aqueous solution. Based on Molecular Dynamics simulations we have characterized the mechanism through which urea stabilizes the collapsed state of PNiPAM in water. Analysis and comparison of the different components of the excess chemical potential of folded and unfolded PNiPAM chains in aqueous urea solutions indicates that enthalpic interactions play no role in stabilizing the collapsed state. We instead find that with increasing urea, solvation of the unfolded state is entropically penalized over solvation of the folded state, thereby shifting the folding equilibrium in favour of the folded state. The unfavourable entropy contribution to the excess chemical potential of unfolded PNiPAM chains results from two urea effects: (1) an increasing cost of cavity formation with increasing urea, (2) larger fluctuations in the energy component corresponding to PNiPAM-(co)solvent attractive interactions. These energy fluctuations are particularly relevant at low urea concentrations (< 3 M) and result from attractive polymer-urea Van der Waals interactions that drive the formation of "urea clouds" but bias the spatial distribution of urea and water molecules with a corresponding reduction of the entropy. We further find indications that urea increases the entropy of the globular state.

1 Introduction

Macromolecules in aqueous solution, such as water soluble polymers or proteins, coexist as an ensemble of folded states (F) in equilibrium with an ensemble of unfolded states (U). The equilibrium $U \rightleftarrows F$ can be perturbed either to the left or to the right by altering the thermodynamic conditions (temperature or pressure) of the medium or by changing the chemical composition of the solution upon addition of chemical compounds. Chemical compounds that shift the equilibrium towards the $F-$ state are called protective osmolytes. They preferentially bind to the $F-$ state, *i.e.* $\Delta\Gamma_{UF} > 0$, as can be understood in terms of the relation

$$\frac{\partial \ln K}{\partial \ln a_c} = \Delta\Gamma_{UF} \qquad (1)$$

introduced by Wyman and Tanford,[1,2] in which K is the equilibrium constant for the above equilibrium, a_c is the activity of the cosolvent in the binary solution and $\Delta\Gamma_{UF} = \Gamma_F - \Gamma_U$, with Γ denoting the preferential binding coefficient. Contrary, denaturants preferentially bind to the $U-$state ($\Delta\Gamma_{UF} < 0$) and shift the equilibrium towards that state.[3,4] The molecular mechanisms that drive preferential binding are important in questions related to protein stability and polymer coil-to-globule transitions; a complete understanding is however still lacking.[5–14]

It is widely accepted that denaturants induce macromolecular unfolding by direct binding of the cosolvent to the surface of the protein. Unfolding is accompanied by an increase of solvent accessible surface area and therefore a larger number of denaturant molecules can interact with the macromolecular surface.[15–17] This mechanism is of enthalpic nature and has been widely supported by both experimental and Molecular Dynamics (MD) simulation studies.[18–20]

Contrary to the enthalpic denaturation mechanism described above, an entropy driven mechanism has been traditionally invoked to explain the stabilization of $F-$ states by protective osmolytes. Protective osmolytes are preferentially depleted from the macromolecular surface leading to preferential protein hydration. Thus, upon folding, the system minimizes the osmolyte-macromolecule excluded volume leading to the effective preferential binding of the osmolyte to the $F-$ state compared to the $U-$ state.[6,21–23] However recent works highlight the role of enthalpy especially for relatively small osmolytes.[24–27] Recent theoretical[28–31] and experimental[32] studies suggest that collapse of macromolecules may be induced by cross-linking or bridging-type interactions between the cosolvent and the monomers. Theoretical studies show that this is the case when the interaction between the polymer and the cosolvent is highly attractive,[28,29,31] while the classi-

[a] *Eduard-Zintl-Institut für Anorganische und Physikalische Chemie and Center of Smart Interfaces, Technische Universität Darmstadt, Alarich-Weiss-Straße 10, 64287, Darmstadt, Germany; E-mail: vandervegt@csi.tu-darmstadt.de*

cal entropically driven depletion mechanism takes place when monomer−cosolvent interactions are weakly attractive.[28]

Sagle *et al.*[32] studied the coil-to-globule transition of Poly(N-isopropylacrylamide) (PNiPAM) in urea and methylated urea aqueous solutions. PNiPAM is a thermoresponsive polymer that undergoes a coil-to-globule transition at 32°C in pure water.[33] The authors found that while urea acts as a protective osmolyte and favors the $F-$ state of PNiPAM, methylated urea derivatives act as denaturant and stabilize $U-$ states. Based on FTIR measurements they proposed a direct folding mechanism where urea forms hydrogen bonds with two neighboring carbonyl groups. Based on Molecular Dynamics simulations, we have recently proposed a mechanism by which direct attractive dispersion Van der Waals urea-PNiPAM interactions confer entropic stability to the $F-$state.[34]

In the present work we want to extend our previous study with the aim of obtaining a thermodynamic description of the mechanism that drives the collapse of PNiPAM by urea. In our previous study we conjectured that attractive Van der Waals dispersion forces of the urea molecules with the hydrophobic isopropyl groups of PNiPAM lead to the formation of a low entropy solvation shell. This picture emerged from previous work where it was shown that preferential urea solvation of hydrophobes is largely energy-entropy compensating.[35] To understand the mechanism that drives the collapse of a polymer chain in the presence of a cosolvent requires comparison of the solvation thermodynamics of, both, the $U-$ and $F-$ states. We have studied the solvation of a PNiPAM chain in the $U-$ and $F-$ states by quantifying the dependence of the enthalpic and entropic components to the PNiPAM excess chemical potential on urea concentration. Our results show that the change of the enthalpic term upon varying the urea concentration is independent of the chain conformation, thus ruling out any mechanism driven by cosolvent bridging. On the other hand, we show that entropic terms resulting from both fluctuations of the attractive interactions and excluded volume effects penalize the $U-$states.

2 Theoretical background

The problem at hand requires to analyse how the urea cosolvent affects the free energy of the $F-$state relative to that of the $U-$state. At any given state point (temperature T, pressure P and urea concentration c_u), the equilibrium $U \rightleftarrows F$ is characterized by the number densities ρ_U and ρ_F of the two conformers in solution whose ratio is determined by the free energy difference ΔF_{UF} between $U-$ and $F-$ states. The equilibrium ratio $K = \rho_F/\rho_U$ is related to ΔF_{UF} by equation 2

$$K = \exp[-\beta \Delta F_{UF}] \tag{2}$$

where $\beta = (k_B T)^{-1}$ with k_B the Boltzmann constant. The free energy difference between the two states vanishes at the lower critical solution temperature (LCST), T_{UF}, of PNiPAM where $\rho_F = \rho_U$. Above the LCST ($T > T_{UF}$), $\rho_F > \rho_U$, while below the LCST ($T < T_{UF}$), $\rho_F < \rho_U$. The cosolvent shifts the equilibrium K_0 in pure water according to[36]

$$K = K_0 \exp[-\beta(\Delta F_{t,F} - \Delta F_{t,U})] \tag{3}$$

where $\Delta F_{t,F} = \mu_F^X - \mu_{F,0}^X$ and $\Delta F_{t,U} = \mu_U^X - \mu_{U,0}^X$ are the transfer free energies of respectively F and U from the pure water solvent to the solvent/cosolvent mixture (Figure 1). The quantities μ^X are the molar excess chemical potentials, which dictate the effect of solvation on processes driven by chemical potential variations.[37] According to equation 3, cosolvent shifts the equilibrium $U \rightleftarrows F$ to the right when $\Delta F_{t,F} < \Delta F_{t,U}$.

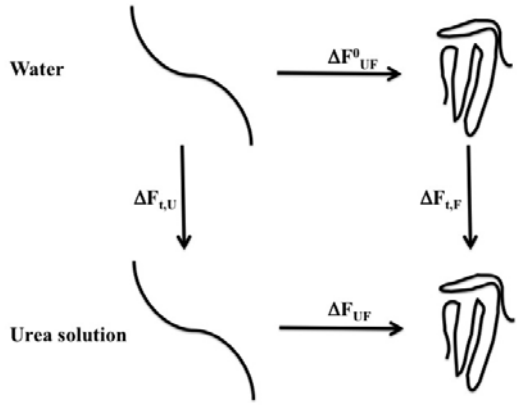

Fig. 1 Thermodynamic cycle used to compute the free energy difference ΔF_{UF} between $U-$ and $F-$ states in urea aqueous solution

In general, osmolytes such as urea may shift the equilibrium $U \rightleftarrows F$ towards the right or the left. In the former case, we deal with a protective osmolyte while in the latter case we deal with a denaturant. Therefore, if

$$(\partial \mu_F^X/\partial c_u) < (\partial \mu_U^X/\partial c_u) \tag{4}$$

we deal with a protective osmolyte, while if

$$(\partial \mu_F^X/\partial c_u) > (\partial \mu_U^X/\partial c_u) \tag{5}$$

we deal with a denaturant.

Application of Kirkwood-Buff theory shows that the cosolvent preferentially binds to the $F-$state over the $U-$state under conditions where equation 4 applies.[38] Under conditions where equation 5 applies, cosolvents instead preferentially bind to the U-state over the F-state.

The preferential binding coefficient in equation 1 is an integral quantity and can therefore not easily be interpreted in terms of structural correlations involving the macromolecules and the cosolvent or solvent molecules. We will here analyze the excess chemical potential, single out contributions to it that have a clear microscopic significance, and use those to discuss molecular driving forces for urea-induced chain collapse. To this end, the excess chemical potential μ^X is written as[39–42]

$$\mu^X = \langle E_{ps} \rangle + \mu^X_{cav} + k_B T \ln \langle \exp(\beta \delta E_{ps}) \rangle_{att} \qquad (6)$$

where $\langle ... \rangle$ denotes averaging over system (polymer+solvent) configurations in the canonical ensemble while $\langle ... \rangle_{att}$ denotes an average over system configurations in which the polymer-solvent energy E_{ps} is attractive. $\delta E_{ps} = E_{ps} - \langle E_{ps} \rangle$ is the polymer-solvent energy fluctuation. The second term (μ^X_{cav}) on the right hand side of equation 6 accounts for cavity formation, while the third term quantifies the reduction of the configuration space volume due to the attractive interactions present in the system.[39,42–44] Assuming linear response, we can write

$$\mu^X = \langle E_{ps} \rangle + \mu^X_{cav} + [\beta/2(\langle E^2_{ps} \rangle - \langle E_{ps} \rangle^2) + ...] \qquad (7)$$

where $\langle E^2_{ps} \rangle - \langle E_{ps} \rangle^2 = \sigma^2_{ps}$ is the variance of the attractive polymer-solvent energy E_{ps}.

We thus see that the excess chemical potential may be written in terms of three contributions. The polymer-solvent enthalpic contribution is determined by Van der Waals and electrostatic interactions between the polymer and the solvent. The cavity contribution μ^X_{cav} is of purely entropic origin and can be related to microscopic density fluctuations in the binary solvent that lead to the formation of empty cavities. The final contribution $\beta \sigma^2_{ps}/2$ accounts for the reduction of configuration space in the presence of fluctuating attractive interactions. We note that this contribution is absent in mean field solvation models.

Application of equations 4 and 7 in molecular simulation studies with frozen $U-$ and $F-$ state conformations provides insight in the role of solvation on the PNiPAM folding equilibrium. The role of the conformational entropy, however, is then not considered. In this work, we will consider frozen as well as fully flexible chain conformations. In the analyses of the simulations with flexible conformations, the energy E_{ps} in the above equations includes the polymer internal potential energy, in addition to the polymer-solvent energy.

3 Methods

Our system consists of a 40-mer PNiPAM chain described according to the OPLS-AA force field[45] solvated in cubic simulation boxes with water and urea. The SPC/E model[46] was used to describe the water while a Kirkwood-Buff based force field derived by Weerasinghe *et al.*[47] was used to represent the urea cosolvent molecules. This force field combination has been previously validated and reproduces T_{UF} in pure water and 5.8M urea concentration in good agreement with experiments.[34,48] Four different urea concentrations, apart from the system in pure water, were considered (Table 1). Systems were simulated at their respective T_{UF}. All simulations were run using the GROMACS 4.5.1. simulation package.[49] A simulation time step of 2 fs was chosen to simulate all systems. All simulations were performed in the isothermal-isobaric ensemble (NpT). Pressure (1 atm.) was kept constant using the he Parrinello-Rahman barostat[50,51] (τ_P = 1.0 ps) while the Nosé-Hoover thermostat[52,53] (τ_T= 0.5 ps) was used to keep the temperature constant. A 12-6 Lennard-Jones potential with a cut-off of 1.40 nm was used to calculate the Van der Waals interactions. Electrostatic interactions have been calculated using Particle-Mesh Ewald method[54] with a real space cut-off of 1.40 nm. Bond lengths atoms were kept at their equilibrium distances using the LINCS algorithm.[55,56] Constraints on all the PNiPAM bonds were applied by using a harmonic potential with a force constant of 1000 kJ mol^{-1} nm^{-2} in all the simulations where the polymer chain was kept frozen. Coordinates were saved every 0.02 ps for subsequent analysis.

Table 1 Number of water (n^{tot}_W) and urea (n^{tot}_U) molecules, average volume (V) and temperature (T) of the systems under study

c_U (mol/l)	n^{tot}_W	n^{tot}_U	V (nm^3)	T (K)
0.0	8548	-	264.75	306.0
0.6	8131	100	259.39	305.0
2.7	6836	400	242.24	301.0
3.8	7135	600	265.45	296.5
5.4	6156	800	250.00	295.0

4 Results

4.1 Preferential urea binding

In a first series of simulations we considered four different urea concentrations in both $U-$ and $F-$ states. We froze three unfolded chains and three folded chains (see Figure 2) and solvated them with the right number of urea and water molecules to reach the target concentrations (see Table 1). These configurations were taken from our previous work.[34] Each resulting system was simulated for 50 ns in the NpT ensemble. Analyses were performed considering the last 40 ns of each simulation.

In our previous work,[34] we showed that the lower folding temperature (LCST) of PNiPAM decreases with increasing urea, hence urea preferentially binds to the folded state

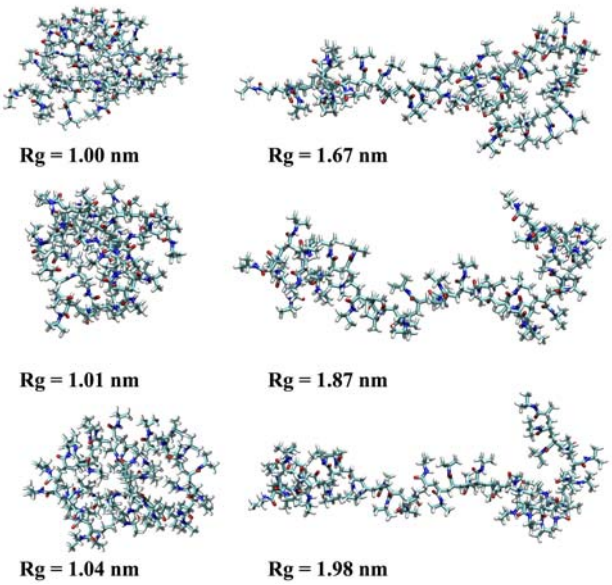

Fig. 2 Snapshots of the investigated folded (left) and unfolded (right) PNiPAM chains.

of PNiPAM in agreement with experimental data.[32] Since the experimental LCST decreases linearly with increasing urea in the urea concentration window considered here (see Table 1), we can approximate $\Delta\Gamma_{UF}$ from the experimental data using[13]

$$\Delta\Gamma_{UF} = \frac{\Delta S^0 \Delta T}{k_B T_0} \tag{8}$$

and use the experimental preferential binding coefficients as further validation of our simulations performed at different urea concentrations. In equation 8, ΔS^0 is the folding entropy in pure water, ΔT is the measured shift of the LCST and T_0 is the LCST in pure water. Using $\Delta S^0 = 40 \times 17$ J mol^{-1} K^{-1},[13] T_0 =305 K, and experimental ΔT-values in the range of urea concentrations between 0.6 M and 5.4 M, we find that $\Delta\Gamma_{UF}$ varies between 0.3 and 2.9. These values are small because urea is a weak binder. We calculated $\Delta\Gamma_{UF}$ from the simulations with frozen conformations but found that the conformation dependency is quite large, hence it is extremely difficult to obtain converged estimates of $\Delta\Gamma_{UF}$.

To characterize the urea distribution around the frozen PNiPAM chain conformations, we calculated the local/bulk partition coefficient (K_p) as defined as

$$K_p = \frac{(\langle n_U \rangle / \langle n_W \rangle)^{local}}{(n_U^{tot} / n_W^{tot})}, \tag{9}$$

where $\langle n_U \rangle$ and $\langle n_W \rangle$ are the average number of respectively urea and water molecules bound to the polymer. n_U^{tot} and n_W^{tot} are respectively the total number of urea and water molecules. Distances are defined as the shortest distance between the center of mass of the urea or water molecule and any atom of the PNiPAM chain. We calculated K_p in equation 9 considering the same set of frozen $U-$ and $F-$ states (Figure 2). Figure 3 shows K_p for the folded and unfolded chains at different urea concentrations. As expected, urea molecules accumulate in the first solvation shell of both $U-$ and $F-$ states, *i.e.* K_p is always greater than 1 in the vicinity of the polymer chain. Furthermore, at all concentrations $F-$states display a slightly higher peak value than the $U-$states, as expected based on the preferential urea binding to the $F-$states. The observed differences between the K_ps corresponding to $U-$ and $F-$ conformations are however quite small. Bigger differences in the K_p between the $U-$ and $F-$ states might be indicative of a conformation dependence on the groups exposed to the urea aqueous solution. However, as we showed in our previous work, the binding interaction of water and urea molecules in the first solvation shell is conformation independent.[34] The magnitude of the peaks decreases with the urea concentration which indicates a more prominent urea accumulation at lower concentrations.

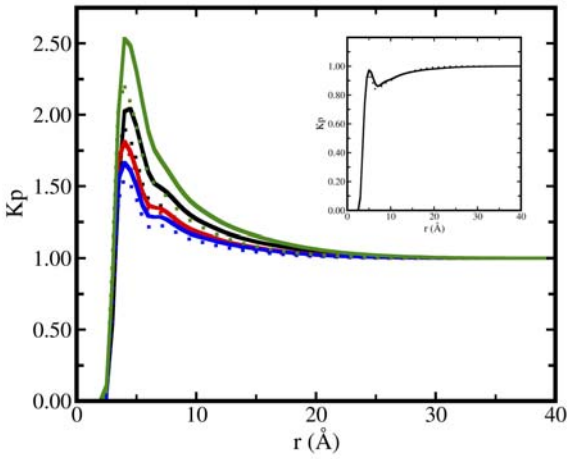

Fig. 3 Average local/bulk partitition coefficient (K_p) as a function of the distance to the frozen polymer in the $U-$state (dotted line) and $F-$ state (continuous line) at 0.6 M (green), 2.7 M (black), 3.8 M (red) and 5.4 M (blue) aqueous urea concentrations. The inset shows the same quantity for the system with 2.7 M urea where attractive Lennard-Jones and electrostatic polymer-solvent interactions have been removed.

From the data in Figure 3 we can conclude that urea accumulates in the first solvation shell of PNiPAM. In proportion to the bulk solvent composition, this observation is most pronounced at low urea concentration. Our previous study[34] showed that urea "clouding" around the PNiPAM chain is

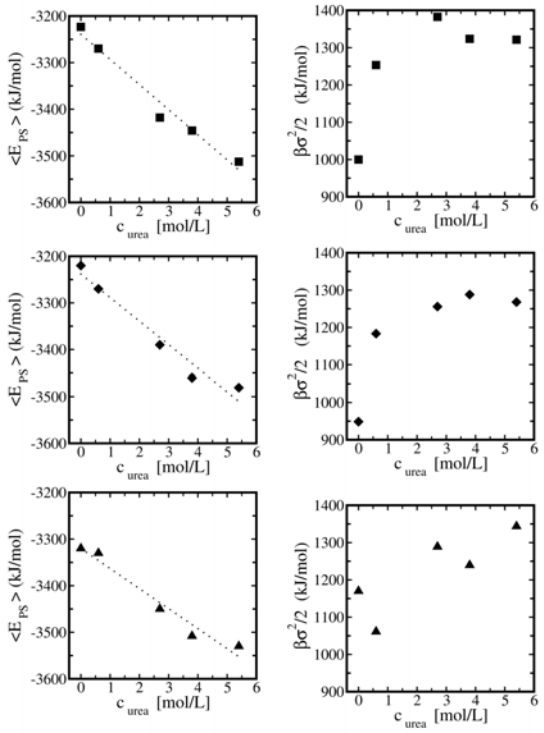

Fig. 4 Solute-solvent energies $\langle E_{ps} \rangle$ (left column) and $(\beta\sigma_{ps}^2/2)$-values (right column) versus urea concentration for the frozen $U-$state PNiPAM conformations with radius of gyration equal to 1.98 nm (■), 1.87 nm (♦) and 1.67 nm (▲). Lines represent linear fits through the data.

driven by favorable Van der Waals interactions with the polymer surface. It remains however quite counterintuitive that despite these favorable direct interactions urea preferentially binds the folded state, *i.e.* the state with the smaller solvent accessible surface area. The molecular mechanism driving the preferential urea binding to the folded state is examined in the next section.

4.2 Statistical thermodynamics analysis

To understand the stabilization of the $F-$ state over the $U-$ state with increasing cosolvent concentration it is necessary to understand not only the solvation of the $F-$ state but also the solvation of the $U-$ state. Urea acts as a protective osmolyte for PNiPAM, so equation 4 must be necessarily satisfied. The chemical potential contains an enthalpic polymer-solvent contribution ($\langle E_{ps} \rangle$) in equations 6 and 7 and an entropic polymer-solvent contribution stemming from cavity formation (μ_{cav}^X) and from fluctuations of the polymer-solvent energy E_{ps} (last term in equation 7).

The sign of the derivative of the cavity chemical potential, $(\partial \mu_{cav}^X / \partial c_u)$, indicates how urea affects the molecular scale flexibility of the binary solvent in terms of its ability to open empty molecular-sized cavities by spontaneous thermal fluctuations. A positive sign indicates that urea suppresses formation of transient cavities, while a negative sign indicates that urea promotes cavity formation. The sign of this quantity can readily be analyzed in the simulations by removing the attractive Lennard-Jones and electrostatic polymer-solvent interactions, while maintaining the repulsive parts of the Lennard-Jones polymer-solvent potential. Application of Kirkwood-Buff theory shows that $(\partial \mu_{cav}^X / \partial c_u) > 0$ provided that the cavity preferentially binds water over urea (cavity is preferentially "wetted"), while the opposite sign is obtained if the cavity instead preferentially binds urea over water.[57] The inset in Figure 3 shows that the PNiPAM cavity is preferentially wetted and therefore the former scenario applies. Indeed, this has also previously been observed in simulations in which the solvation of hydrocarbon cavities in urea-water mixtures has been examined, and where it was moreover found that larger cavities are stronger preferentially wetted in comparison with smaller cavities.[58] Stronger preferential wetting leads to a larger positive derivative, $(\partial \mu_{cav}^X / \partial c_u) > 0$, opposing solvation.[57] The macroscopic counterpart of this observation is that urea increases the surface tension of water. We thus conclude that the entropy penalizes solvation of the $U-$ state stronger than solvation of the $F-$ state with increasing urea, *i.e.* the entropic cost of cavity formation provides driving force that stabilizes the $F-$ state, which occupies a smaller cavity.

The role of the polymer-solvent energy in stabilizing the $F-$ state can be examined by computing the derivatives $(\partial \langle E_{ps}^U \rangle / \partial c_u)$ and $(\partial \langle E_{ps}^F \rangle / \partial c_u)$. Only when the inequality $(\partial \langle E_{ps}^F \rangle / \partial c_u) < (\partial \langle E_{ps}^U \rangle / \partial c_u)$ is satisfied, enthalpic interactions play a role in stabilizing the folded state. If on the other hand the folding mechanism is entirely entropy-driven the inequality $(\partial[(\beta\sigma_{ps}^2/2) + \mu_{cav}]_F / \partial c_u) < (\partial[(\beta\sigma_{ps}^2/2) + \mu_{cav}]_U / \partial c_u)$ must be met. Since we know that urea promotes the folding of PNiPAM chains, to answer our question we need to discern which of these two inequalities is true. Firstly, to cancel out any possible contribution coming from the conformational fluctuations of the polymer chain on the enthalpic and/or entropic terms, we have determined the variation of $\langle E_{ps} \rangle$ and $(\beta\sigma_{ps}^2)/2$ versus urea concentration for selected frozen $U-$ and $F-$ states shown in Figure 2. Figures 4 and 5 show the data for the three different coils and three different globules, respectively.

$\langle E_{ps} \rangle$ decreases linearly with urea concentration for the three considered $U-$ and $F-$ configurations. $(\partial \langle E_{ps}^U \rangle / \partial c_u)$ is slightly lower than $(\partial \langle E_{ps}^F \rangle / \partial c_u)$. In the system with $R_g =$ 1.00 nm, $\langle E_{ps} \rangle$ has not been converged and presents a greater slope. The value of the slopes obtained from fitting the points in a linear regression are presented in Table 2. These results suggest that the enthalpic term slightly penalizes the $F-$ state

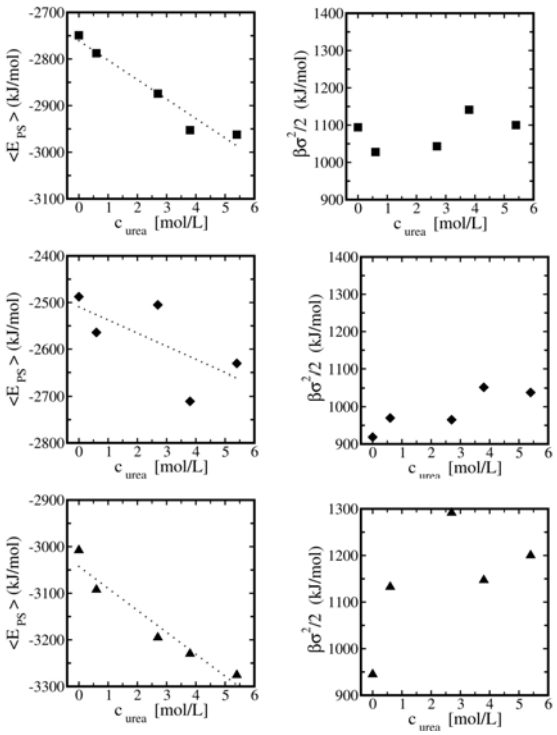

Fig. 5 Solute-solvent energies $\langle E_{ps} \rangle$ (left column) and $(\beta\sigma_{ps}^2/2)$-values (right column) versus urea concentration for the frozen $F-$state PNiPAM conformations with radius of gyration equal to 1.04 nm (■), 1.00 nm (♦) and 1.01 nm (▲). Lines represent linear fits through the data.

in favor of the $U-$ state. The dependence of the entropy contribution $(\beta\sigma_{ps}^2/2)$ on urea concentration in the right panels of figures 4 and 5 clearly shows that the $U-$ state is increasingly penalized with urea concentration at lower urea concentration (c_u = 0.6 M) where the urea clouds are more prominent, *i.e.* the concentration where K_p shows the largest maximum (Figure 3). This is especially remarkable for the more stretched configurations (R_G = 1.98 nm and 1.87 nm). Since the slope of the cavity contribution μ_{cav} is expected also to be larger for the $U-$ state than for the $F-$ state we conclude that urea shifts the equilibrium $U \rightleftarrows F$ in favour of F by entropically penalizing U.

The data we have discussed up to now provides quantitative support for the entropic folding mechanism we postulated in our previous work.[34] However in reality the conformation of the polymer chain is expected to fluctuate. The effect of chain flexibility is quantified here by the contribution of the polymer-polymer potential energy and the corresponding energy fluctuations in chain excess chemical potential. To this end, we have run a set of 45 ns long MD simulations starting from the frozen configurations but allowing the chain to

Table 2 Slopes of the linear fits of $\langle E_{ps} \rangle$ versus urea concentration for all the systems under study. For the flexible systems R_G is the radius of gyration of the initial configuration.

R_G(nm)	$\partial\langle E_{ps}\rangle/\partial c_u$ frozen	$\partial\langle E_{ps}\rangle/\partial c_u$ flexible
1.98	-54	-71
1.87	-50	-70
1.67	-43	-61
1.04	-42	-45
1.00	-28	-66
1.01	-47	-67

Table 3 Slopes of the linear fits of $(\beta\sigma_{ps}^2/2)$ versus urea concentration for all the systems under study. For the flexible systems R_G is the radius of gyration of the initial configuration.

R_G(nm)	$\partial(\beta\sigma_{ps}^2/2)/\partial c_u$ frozen	$\partial(\beta\sigma_{ps}^2/2)/\partial c_u$ flexible
1.98	47	67
1.87	49	-20
1.67	41	103
1.04	10	-93
1.00	21	-60
1.01	36	-103

fluctuate, *i.e.* turning off the constraints used to keep the polymer chain frozen. We have used the last 40 ns for analysis. It is worth mentioning that only those configurations with a $R_G > 1.50$ nm have been considered as $U-$ states while only those configurations with a $R_G < 1.10$ nm have been considered as $F-$ states. Figures 6 and 7 show respectively the results for the flexible U and F conformations. For the flexible polymers $(\partial\langle E_{ps}^F\rangle/\partial c_u) \approx (\partial\langle E_{ps}^U\rangle/\partial c_u)$ (Table 2). Hence, we again find that enthalpic interactions play no role in shifting the PNiPAM folding equilibrium. The only observed exception is the system starting at $R_G = 1.04$ nm, which seems not to converge. In this system, the compact $F-$ state starts unfolding reaching values of $R_G \approx 1.10$ nm.

Removing the chain flexibility constraints affects the entropic contribution $(\partial(\beta\sigma_{ps}^2/2)/\partial c_u)$ to the chemical potential variation, especially for the collapsed $F-$ states where $(\partial(\beta\sigma_{ps}^2/2)/\partial c_u)$ now has a negative sign (Table 3). This indicates that folded globules in urea solution have larger entropy than folded globules in pure water (assuming that their excluded volumes are the same). Because the energy fluctuations σ_{ps}^2 are smaller in urea solution than in water, the potential energy surface of the globule is flattened out by urea. This may have several implications and we plan to investigate this aspect in greater detail in a future publication. Note that for the $U-$ states, the corresponding effect of removing the chain flexibility constraints is smaller (except for the system starting at $R_G = 1.87$ nm). Consequently, combined effects of chain flexibility and solvation in urea solution entropically pe-

nalize the $U-$state and provide driving force for shifting the PNiPAM folding equilibrium towards the folded state.

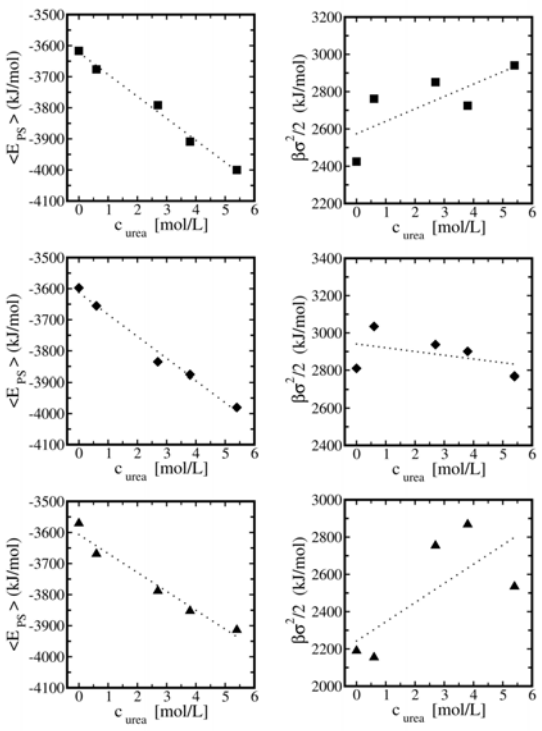

Fig. 6 Solute-solvent energies $\langle E_{ps}\rangle$ (left column) and $(\beta\sigma_{ps}^2/2)$-values (right column) versus urea concentration for flexible PNiPAM conformations with initial radius of gyration equal to 1.98 nm (■), 1.87 nm (♦) and 1.67 nm (▲). Lines represent linear fits through the data.

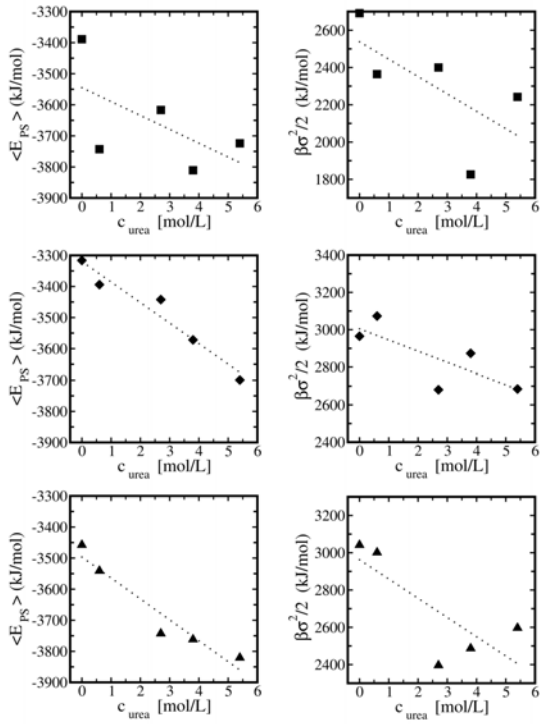

Fig. 7 Solute-solvent energies $\langle E_{ps}\rangle$ (left column) and $(\beta\sigma_{ps}^2/2)$-values (right column) versus urea concentration for flexible PNiPAM conformations with initial radius of gyration equal to 1.04 nm (■), 1.00 nm (♦) and 1.01 nm (▲). Lines represent linear fits through the data.

5 Conclusions

The effect of urea on the coil-globule folding equilibrium of PNiPAM in aqueous solution, studied in earlier work,[34] has been further explored in this paper with molecular dynamics simulations at different urea concentrations. The simulation trajectories obtained at different urea concentrations have been used to perform a detailed thermodynamic analysis of the molecular driving forces for urea induced collapse. The results obtained in this work support and complement the entropic mechanism postulated earlier.[34]

Urea shifts the equilibrium between coil and globular states in favour of the globular state (*i.e.* urea "salts out" the polymer) despite attractive urea-polymer Van der Waals interactions in the first solvation shell of the macromolecule.[34] This observation is counter-intuitive. Based on a simple solvent accessible surface argument the opposite effect ("salting in") is expected. Hence, the naturally emerging question is whether urea binds stronger to globular state as compared to the coil state though, *e.g.* bridging interactions, or some other mechanism?

The results presented in this paper are based on a statistical mechanics analysis of the PNiPAM chemical potentials in the coil and globular states. We find that urea-induced hydrophobic collapse is caused by two reinforcing entropic mechanisms: (1) cavity formation penalizes the coil state stronger than the globular state with increasing urea, (2) accumulation of urea around frozen chain conformations entropically penalizes the coil state stronger than the globular state with increasing urea at concentrations below approximately 3 M. The polymer-solvent energy instead decreases favourably with increasing urea concentration, however this decrease in energy occurs with approximately similar rates for both the coil and globular states. Hence, enthalpic effects play no role in stabilizing the globular state. Although specific interactions (such as bridging) may occur in the globular state, these interactions are unlikely to contribute in stabilizing the globule.

Mean field polymer physics models fail to describe polymer collapse induced by attractive cosolvent. The present

results indicate that this may be caused by solvent compositional dependencies of the excluded volume (cavity) entropy as well as by energy fluctuations, both not acounted for in such models. Importantly, extension of these models with enthalpic terms (that, for example, account for bridging interactions[31]) needed to overcome the loss of conformational entropy upon collapse, may lead to an ambiguous physical picture of cosolvent-induced polymer collapse, in particular for weakly interacting cosolvents, such as urea but also methanol.

We finally point out that the herein observed entropic driving force for collapse may vanish in non-ideal cosolvent-water mixtures. Previous simulation studies of the solvation of nonpolar molecules in cosolvent-water mixtures have shown that the entropic cavity formation penalty is larger in urea-water mixtures than in pure water.[35] This effect is however reversed in nonideal cosolvent-water mixtures with cosolvents that typically are slightly amphiphilic and contain hydrophobic groups.[35] In these systems, cavity formation occurs predominantly in microscopic regions with locally higher cosolvent concentrations (cosolvent "clusters").[59] In the present context of polymer folding equilibria, this may lead to a situation in which increasing cosolvent causes a smaller opposing entropy contribution and a larger favouring energy contribution that eventually causes the folding equilibrium to shift in favour of the unfolded polymer. This scenario would explain why methylated urea has exactly the opposite effect than urea and unfolds PNiPAM chains.[32]

6 Acknowledgements

This research was supported by the German Research Foundation (DFG) within the Cluster of Excellence 259 Smart Interfaces - Understanding and Designing Fluid Boundaries. The authors would like to express their gratitude to the Hochschulrechenzentrum at the TU-Darmstadt for the computational time provided.

References

1 J. Wyman, *Adv. Protein Chem.*, 1964, **19**, 223 – 286.
2 C. Tanford, *J. Mol. Biol.*, 1969, **39**, 539 – 544.
3 P. Yancey, M. Clark, S. Hand, R. Bowlus and G. Somero, *Science*, 1982, **217**, 1214–1222.
4 J. A. Schellman, *Annu. Rev. Biophys. Biophys. Chem.*, 1987, **16**, 115–137.
5 K. A. Dill, *Biochemistry*, 1990, **29**, 7133–7155.
6 S. N. Timasheff, *Annu. Rev. Biophys. Biomol. Struct.*, 1993, **22**, 67–97.
7 Q. Zou, B. J. Bennion, V. Daggett and K. P. Murphy, *J. Am. Chem. Soc.*, 2002, **124**, 1192–1202.
8 B. M. Baysal and F. E. Karasz, *Macromol. Theory Simul.*, 2003, **12**, 627–646.
9 T. O. Street, D. W. Bolen and G. D. Rose, *Proc. Natl. Acad. Sci. USA*, 2006, **103**, 13997–14002.
10 Y. Zhang and P. S. Cremer, *Annu. Rev. Phys. Chem.*, 2010, **61**, 63–83.
11 J. L. England and G. Haran, *Annu. Rev. Phys. Chem.*, 2011, **62**, 257–277.
12 D. R. Canchi and A. E. García, *Annual Review of Physical Chemistry*, 2013, **64**, 273–293.
13 J. Heyda and J. Dzubiella, *J. Phys. Chem. B*, 2014, **118**, 10979–10988.
14 P. Jungwirth and P. S. Cremer, *Nat. Chem.*, 2014, **6**, 261–263.
15 E. P. K. Hade and C. Tanford, *J. Am. Chem. Soc.*, 1967, **89**, 5034–5040.
16 H. Inoue and S. N. Timasheff, *J. Am. Chem. Soc.*, 1968, **90**, 1890–1897.
17 G. I. Makhatadze and P. L. Privalov, *J. Mol. Biol.*, 1992, **226**, 491 – 505.
18 L. Hua, R. Zhou, D. Thirumalai and B. J. Berne, *Proc. Natl. Acad. Sci. USA*, 2008, **105**, 16928–16933.
19 W. K. Lim, J. Rösgen and S. W. Englander, *Proc. Natl. Acad. Sci. USA*, 2009, **106**, 2595–2600.
20 D. R. Canchi, D. Paschek and A. E. García, *J. Am. Chem. Soc.*, 2010, **132**, 2338–2344.
21 S. Asakura and F. Oosawa, *J. Chem. Phys.*, 1954, **22**, 1255–1256.
22 J. C. Lee and S. N. Timasheff, *J. Biol. Chem.*, 1981, **256**, 7193–7201.
23 T. Arakawa and S. N. Timasheff, *Biophys. J.*, 1985, **47**, 411–414.
24 R. Gilman-Politi and D. Harries, *J. Chem. Theory Comp.*, 2011, **7**, 3816–3828.
25 X. Li and G. C. Schatz, *J. Phys. Chem. Lett.*, 2013, **4**, 2885–2889.
26 S. Sukenik, L. Sapir and D. Harries, *Curr. Opin. Coll. Interf. Sci.*, 2013, **18**, 495 – 501.
27 L. Sapir and D. Harries, *J. Phys. Chem. Lett.*, 2014, **5**, 1061–1065.
28 J. Heyda, A. Muzdalo and J. Dzubiella, *Macromolecules*, 2013, **46**, 1231–1238.
29 J. Mondal, G. Stirnemann and B. J. Berne, *J. Phys. Chem. B*, 2013, **117**, 8723–8732.
30 D. Mukherji and K. Kremer, *Macromolecules*, 2013, **46**, 9158–9163.
31 D. Mukherji, C. M. Marques and K. Kremer, *Nat. Commun.*, 2014, **5**, 4882.
32 L. B. Sagle, Y. Zhang, V. A. Litosh, X. Chen, Y. Cho and P. S. Cremer, *J. Am. Chem. Soc.*, 2009, **131**, 9304–9310.
33 M. Heskins and J. E. Guillet, *J. Macromol. Sci. - Part A Chem.*, 1968, **2**, 1441–1455.
34 F. Rodríguez-Ropero and N. F. A. van der Vegt, *J. Phys. Chem. B*, 2014, **118**, 7327–7334.
35 N. F. A. van der Vegt, D. Trzesniak, B. Kasumaj and W. F. van Gunsteren, *ChemPhysChem*, 2004, **5**, 144–147.
36 C. Tanford, *J. Am. Chem. Soc.*, 1964, **86**, 2050–2059.
37 A. Ben Naim, *Solvation Thermodynamics*, Plenum Press, New York, 1987.
38 V. Pierce, M. Kang, M. Aburi, S. Weerasinghe and P. Smith, *Cell. Biochem. Biophys.*, 2008, **50**, 1–22.
39 I. C. Sanchez and T. M. a. Truskett, *J. Phys. Chem. B*, 1999, **103**, 5106–5116.
40 P. Schravendijk and N. F. A. van der Vegt, *J. Chem. Theory Comp.*, 2005, **1**, 643–652.
41 D. Ben-Amotz, F. O. Raineri and G. Stell, *J. Phys. Chem. B*, 2005, **109**, 6866–6878.
42 N. F. A. van der Vegt, M.-E. Lee, D. Trzesniak and W. F. van Gunsteren, *J. Phys. Chem. B*, 2006, **110**, 12852–12855.
43 G. Graziano, *J. Phys. Chem. B*, 2001, **105**, 2632–2637.
44 F. Taherian, F. Leroy and N. F. A. van der Vegt, *Langmuir*, 2013, **29**, 9807–9813.
45 W. L. Jorgensen and J. Tirado-Rives, *J. Am. Chem. Soc.*, 1988, **110**, 1657–1666.
46 H. J. C. Berendsen, J. R. Grigera and T. P. Straatsma, *J. Phys. Chem.*, 1987, **91**, 6269–6271.
47 S. Weerasinghe and P. E. Smith, *J. Phys. Chem. B*, 2003, **107**, 3891–3898.
48 J. Walter, V. Ermatchkov, J. Vrabec and H. Hasse, *Fluid Phase Equilib.*, 2010, **296**, 164 – 172.
49 B. Hess, C. Kutzner, D. van der Spoel and E. Lindahl, *J. Chem. Theory*

Comput., 2008, **4**, 435–447.
50 M. Parrinello and A. Rahman, *J. Appl. Phys.*, 1981, **52**, 7182–7190.
51 S. Nosé and M. Klein, *Mol. Phys.*, 1983, **50**, 1055–1076.
52 S. Nosé, *Mol. Phys.*, 1984, **52**, 255–268.
53 W. G. Hoover, *Phys. Rev. A*, 1985, **31**, 1695–1697.
54 T. Darden, D. York and L. Pedersen, *J. Chem. Phys.*, 1993, **98**, 10089–10092.
55 B. Hess, H. Bekker, H. J. C. Berendsen and J. G. E. M. Fraaije, *J. Comp. Chem.*, 1997, **18**, 1463–1472.
56 B. Hess, *J. Chem. Theory Comput.*, 2008, **4**, 116–122.
57 N. F. A. van der Vegt and W. F. van Gunsteren, *J. Phys. Chem. B*, 2004, **108**, 1056–1064.
58 D. Trzesniak, N. F. A. van der Vegt and W. F. van Gunsteren, *Phys. Chem. Chem. Phys.*, 2004, **6**, 697–702.
59 M.-E. Lee and N. F. A. van der Vegt, *J. Chem. Theory Comp.*, 2007, **3**, 194–200.